Towards the integration of air chemistry and building simulation models IAQ assessment

Jeroen van 't Ende [a, b], *Mihalis* Lazaridis [b], *Christian* Struck [a], *Annemarie* Weersink [a]

[a] Chair of Sustainable Building Technology, School of Business, Buildings & Technology, Saxion University of Applied sciences, Enschede, the Netherlands, j.a.n.vantende@saxion.nl.

[b] Faculty of Environmental Engineering, Technical University of Crete, Chania, Greece.

Abstract. To limit greenhouse gas emissions, energy efficiency measures are applied at a large scale resulting in buildings becoming more airtight. Indoor environmental quality depends strongly on ventilation rates. Whilst controlled ventilation contributes to the reduced use of fossil fuel, too little ventilation increases the risk of health-damaging concentrations of pollutants in the indoor environment. There are three primary sources for pollutants indoors (1) ventilated outside air, (2) emissions from activities such as cooking and cleaning and (3) longitudinally emitted pollutants from people, building components and furnishings. Some accepted primary pollutants to assess indoor air quality are CO2, Volatile Organic Compounds (VOC) and OH. However, indoor chemistry studies indicate the presence of a great amount of complementary secondary pollutants with potentially health-damaging effects. Secondary pollutants indoors are the result of chemical reactions of pollutants with solar radiation as an energy source and ozone/other oxidants. Little is known about the type of resultant secondary pollutants and their effect on human health. One approach to assess the effect of secondary pollutants on indoor environmental quality is to integrate chemical box models with building simulation models, e.g. computational fluid dynamics. In this contribution, the authors provide an overview of the state of the art in integrated simulation models of air chemistry with building performance. A reduced-order case study will be presented comparing methods and identifying key parameters for indoor air quality, including selected secondary pollutants. Additionally, a conceptual framework is presented for assessing the impact of secondary pollutants on human health.

Keywords. CFD, Adverse health effects, simulation, breathing, mannequin

1. Introduction

In atmospheric models, chemical models such as Master Chemical Mechanism (MCM) [5] can be used to describe the breakdown of compounds in the open atmosphere. A tool like [1] combined with [19] can easily run "chamber" experiment simulations. In indoor air quality assessments, such models are not available and detailed chemical analysis, in general, is not applied. The current state of indoor air quality and key priorities to focus on were identified by [9], among others, it was found that indoor gas-, solid- and liquid-phase chemistry potential needs to be assessed. In the European Union (EU) VOC are defined as:

"VOC shall mean any organic compound having at 293,15 K a vapour pressure of 0,01 kPa or more, or having a corresponding volatility under the particular conditions of use."[2]. The standards used are similar but still widely different, there is no agreement on what VOC exactly are. One example,

formaldehyde, is considered to have strong adverse health effects and is also measurable in most indoor environments. This pollutant is primarily emitted by furniture, glues, paints, resins and wood.

Human activities such as sports, cooking and cleaning will also cause increased levels of pollutants. When using liquid cleaning agents to clean the floor, a large surface area is covered in a thin film. This promotes evaporation of the cleaning agent. Limonene is commonly used as a solvent in cleaning products, therefore this is a realistic scenario. It is also used as a flavouring agent and is known as the "fragrance" of oranges. In [12] an experiment has been conducted under controlled conditions: the limonene concentration and reaction products under oxidative stress of ozone are simulated through a Computational Fluid Dynamics (CFD) package. To gain more information about the healthiness of indoor air, toxicological databases are available. This combined with known reaction constants and pathways for breakdown makes it

possible to simulate these effects on a relatively small scale.

1.1 Research objective

The objective is to specify a way to translate the air chemical content to a health effect index. One objective(s) that can be distilled from above is: to provide a methodology to study indoor gas-phase chemistry. This includes primary pollutants introduced by ventilation (or surface emissions) and secondary pollutants introduced through chemical reactions. This is one of the main concerns of this effort.

1.2 Species of interest

Lower Ozone concentrations are found indoors compared to the outdoor environment [14], therefore it is an interesting gas to monitor that is likely involved in the breakdown of VOC. Furthermore, Limonene is studied because it is widely available. Since the Smart Tiny Lab (STL) building is new, it is suspected that formaldehyde is being emitted from new building materials like Oriented Strand Board (OSB). The methodology described will be limited to the chemicals **Limonene**, **Ozone** and **Formaldehyde** bur is not limited to these chemicals, it is applicable in a wider context.

2. Literature

In classical terms, Indoor Air Quality (IAQ) is defined as a combination of temperature, humidity and (chemical) pollution. In terms of pollution, it is common to look at CO2 or VOC concentrations. Open Field Operation And Manipulation (OpenFOAM) [21] can be used to model air. OpenFOAM has many built-in solvers and examples, the general workflow is to find an example that is close to your problem and adjust a copy of the example case to your custom case. For more advanced problems, the solver can be changed/rewritten. Depending on what you want to simulate, different simplifications can be made. OpenFOAM does this by providing the end-user with different solvers which are set up for specific simplifications such as incompressible flow, no heat transfer, particle tracking, transient or steady-state, multi-species, combustion, chemical reactions and more.

2.1 CFD model

The most sophisticated models applied here, use the rhoReactingBuoyantFoam "standard application" from OpenFOAM. This is a multi-species, density-based solver which supports chemistry.

A Reynolds-averaged-Simulation (RANS) with K-epsilon model is used for Momentum transport, this model can be applied when the phenomena of interest are far away from turbulent phenomena. All eddies are averaged out. So make sure that Reynolds numbers are low, and well in the laminar region. Or make sure that the turbulent phenomena do not matter.

2.2 Material emissions

In [18] different sources of formaldehyde are identified and investigated with Monte-Carlo methods. The generated normal distributions can be used to assign emissions to wall elements in the room model. Wall coverings have been found to emit $0.5 \frac{\mu g}{m^2 h}$. For OSB material mean emissions of $43 \frac{\mu g}{m^2 h}$ have been found. Since the structure is well known, these emissions can be taken into account. In [12], chemical equation (1) is used, all reaction products are summarized in C_{prod}.

$$C_{10}H_{16} + O_3 = C_{prod} \qquad (1)$$
$$k(T) = Ae^{\frac{-B}{T}} \left(\frac{T}{300}\right)^n \qquad (2)$$

The Arrhenius equation (2) and the following constants $A = 1.752e^{-15} [cm^3 mole^1 s^{-1}]$, $B = 0$ and $T = 770$ allow for accurate concentration profiles. See Chapter 3 for more details. The Arrhenius rate constants are found in [15]. Note that the found A value has to be converted through Avogadro's constant: $N_a = 6.022141 \cdot 10^{23} [mol^{-1}]$ to work correctly with OpenFOAM.

2.4 Respiration model

For the second simulation shown in chapter 3.2, A breathing model needs to be incorporated. The mannequin generating tool DINED [4] is suitable for generating the required 3D geometry. The tool allows the user to generate a realistic 3D human model based on a large number of 3D scans.
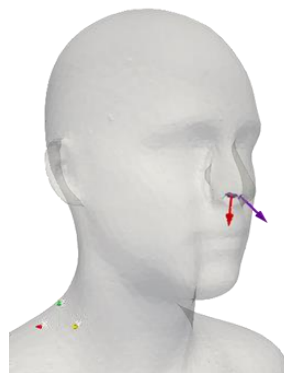

Fig. 1 - Normal vectors for the involved flow areas, respectively: $4.47332 \cdot 10-5[m2]$ of the left, purple area. and $2.38476 \cdot 10-5[m2]$ for the right, red area.

Since the 3D models generated by DINED are realistic, the existing geometry around the nose can be used to determine the involved flow areas. This is shown in **Fig. 1.** The total flow-area, from and to which the breathing occurs needs to be combined with a changing speed vector. The combination of these will lead to airflow in $[L \cdot min^{-1}]$. The total "breathing" area is $4.47332 \cdot 10^{-5} + 2.38476 \cdot 10^{-5} = 6.85808 [m^2]$

This airflow should line up with standard figures that can be found for normal human breathing under rest conditions [8]. The breathing volume per minute ranges from $6[L]$ to $8[L]$ per minute. The average adult takes 12-15 breaths per minute [8]. The breathing rate has been set to 0.23 Hz, which equals $1/0.23 = 4.34$ seconds for one breathing cycle, and $60/4.34 = 13.8[breaths \cdot min^{-1}]$. Combining all the above characteristic numbers, a simple breathing model was made and has been visualized in **Fig. 2**, the green line shows the accumulated exhaled air over one minute, where the red and blue lines show the inhalation rate, and total breathing cycle rate. The last value of the green line,

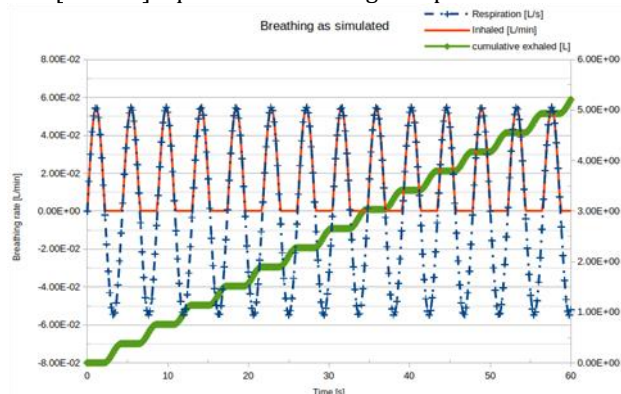$5.37[L \cdot min^{-1}]$ equals the breathing rate per minute.

Fig. 2 - Breathing rate as simulated in OpenFOAM with a target volume of $650[L \cdot min^{-1}]$.

2.5 Toxicity indexes

With toxicological dose descriptors, the relationship between effects and the dose is described. To describe different effects, different dose descriptors have been called into life by toxicologists. Some important ones are:

1. Lethal Concentration 50% (LC50) in $[mg \cdot L^{-1}]$ or $[ppm]$ and sometimes $[mg \cdot L^{-1} \cdot 6h^{-1} \cdot day^{-1}]$. These values are used for gases.

2. No Observed Adverse Effect Level (NOAEL) or *NOAEC* for gases.

3. Lowest Observed Adverse Effect Level (LOAEL) or *LOAEC* for gases.

Repeated dose Toxicity tests provide valuable information about chemicals. NOAEL or LOAEL can be derived and specific target organ toxicity can be determined. In **Tab. 1,** 6 categories of toxicity tests are given, in general, the above-mentioned dose descriptors can be categorized under one of those 6 categories.

Data availability

One of the biggest challenges in IAQ and toxicology is the vast amount of chemicals from which the exact properties are required. The availability of good and reliable measurements varies widely from species to species and in general data availability is sparse, unless it concerns a common species. Nonetheless,

multiple systems try to index all available information, the following list shows sources that have been consulted and proved useful.

1. Pubchem [17] and Pubmed [7] contain chemical and medical information for most species.

2. Eurochamp [3] contains gas-phase reaction-rate constants.

3. Comptox [22] Computational toxicology chemicals dashboard.

4. GenRA [11] Generates Read-Across predictions by looking at properties of nearest k neighbours.

In particular, the GenRA tool is very useful, it can generate predictions of toxicological values by looking at similar chemicals. This is *not* accurate or realistic, but most probably better than a random guess. To generate a ReadAcross prediction for a given compound, the following steps are taken with genRA:

1. select the chemical of interest (in this example Ozone)

2. Evaluate the proposed analogues and check data availability from different databases

3. Data gap analysis, possibly filter analogues that contradict the majority

4. generate genRA prediction for the chemical of interest and export data

It is expected that with time, the predictions of genRA will improve if new measurements of toxicological effects are continued to be added to the database. This means that this method of calculating a health index will also gain some accuracy.

2.6 Health index calculation method

In the GenRA [11] database, the effect types as shown in **Tab. 1** can be found. These effects cannot be ranked on *severity*, since there is an overlap between effects. Still, it is clear to see that the long-term consequences of **MGR** effects are by far the worst. The first 3 effects can "cross" to offspring, which gives it a higher score. Where **CHR** is the worst for the individual according to this created rating. The severity rating will later be used as a weight to scale to the total.

Tab. 1 - Toxicity testing types normally used to determine Derived No Effect Levels.

Effect types	severity	Explanation
MGR	1	Multigenerational reproductive toxicity
REP	0.9	reproduction/developmental toxicity

DEV	0.8	Prenatal Developmental toxicity	
CHR	0.7	Chronic toxicity	
SUB	0.6	Subchronic toxicity	
SAC	0.5	Sub-acute repeat dose toxicity	

For each of the mentioned types in **Tab. 1**, there are between 1 to 129 different toxicity effects defined, ranging from specific organ toxicity to death.

It is good to realize that there is a lot of information behind the 6 categories in 2.1, note that *none* of the effect types has all 129 effects defined, this is a product of the subset that has been selected. Most predictions have high p-values and are not considered significant, p-values might go down in the future when more measurements are added to the database.

Overall values will be calculated for the 6 categories and per gas. The Adverse Effect Index (AEI), AEI_{test} value essentially consists of 3 calculated values.:

1. A reliability weight to compensate for low data availability, and thus more uncertainty.

2. A positive-test weight to incorporate the predicted values from genRA.

3. The severity weight(s),$S_{gas,test}$, mentioned **Tab. 1** to account for the range of severeness.

$$\eta_{gas,test,rel} = \frac{129}{Tox_{gas,test,available}} \qquad (3)$$

The reliability weights are calculated through equation (3). The total amount of effects for $Tox_{O3,CHR,available}$ would be 101 according to figure 2.4, the 129 comes from the maximum amount of tests possibly available in the genRA database.

$$P_{gas,test} = \frac{Tox_{gas,test,available}}{\Sigma(Tox_{gas,test,magnitude})} \qquad (4)$$

The positive-test weights are calculated in equation (4) The total amount of effects for the test category and gas are divided by the sum of available magnitudes for the same combination of gas and test. With the above example into consideration, the weight would become: $P_{O3,CHR} = \frac{101}{...+0.872+...}$ where *0.872* is part of the sum.

$$AEI_{gas,test} = P_{(gas,test)} \cdot S_{gas,test} \cdot \eta_{gas,test,rel} \quad (5)$$

Now the 3 weights can be multiplied as shown in equation (5) and all $AEI_{gas,test}$ can be calculated.

$$x_i = \frac{X_{max}-X_i}{X_{\max}-X_{min}} \qquad (6)$$

As the last step, the found weights will be normalized through equation(6), where X_{max} and X_{min} will be taken from all found $AEI_{gas,test}$.

2.7 Health index concept result

An example matrix where the above method was applied is shown in **Fig. 13**, the matrix represents the strength of the effect type definitions from **Tab. 1**. The matrix has been normalized because this method relies on working with non-physical weights, for this to work, concentration data also needs to be normalized before being post-processed with this matrix.

The steps are as follows to apply this matrix to a CFD simulation where gas concentrations are available:

1. Normalize the CFD gas concentrations through equation (6).

2. Normalize over the time of interest (multiple time steps, larger set for finding X_{max} and X_{min}) or only one timestep of interest.

3. Multiply the normalized concentrations with the coefficients for the same gas, do this per *Effectgroup*/test.

4. A positive-test weight to incorporate the predicted values from genRA.

5. The weight(s),$S_{gas,test}$, mentioned in table 2.1 to account for the range of severeness.

6. Take the average of the *Effectgroups* per gas, this gives you a total health index on gas-level.

7. Take the average of all the gas-level health indexes for a specific location and a true AEI index is defined.

8. As a final step, the average for a complete simulation/space can be taken to get a total average.

It is important to be aware of the limitations of this technique, no absolute *limits* or *concentrations* are calculated so it should not be used to determine absolute limits. It can be used to assess the *relative* healthiness of different locations within the same space, simulation, or at least under very similar conditions. The current categorization can be improved by expert knowledge, the scripts used for generating above have taken this into account and can easily be adjusted to alternate categorization schemes.

3. Experiments

2 Simulations have been conducted with OpenFOAM .org Version 9. The first simulation is briefly shown below in **Fig. 3**. The shown simulation involves A coarse human breathing model The mannequin is used to study the effects of humans on indoor air.

At the Saxion university of applied sciences, a test room is available. Limonene concentration from cleaning activities will be simulated and Formaldehyde emissions from the building materials.
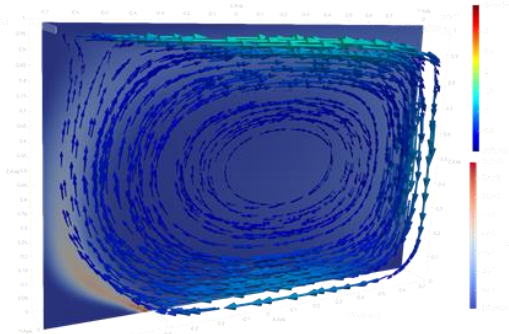
Fig. 3 - Geometry overview of the reproduced case study [12]

The case study presented in [12] has successfully been repeated with similar results. Proving that the chosen toolchain, OpenFOAM and ParaView are capable of solving similar problems. Reaction constants have been retrieved from [15]

3.2 Smart tiny lab summary

It has been established in chapter 3.1 that the developed model is adequately accurate to approach indoor species concentrations. In this chapter, the details of the case study will be shown

A building for testing the integration and overall performance of building coupled installations and IAQ test lab has recently been built at the Saxion University of Applied Sciences.

A mesh model of the STL for CFD purposes has been created initially with a 5 cm grid-scale. There are no simplifications in terms of 2D-case or mirroring possible within the room. The test chambers are geometrically identical, so results can be mirrored for the right test room (room 2). A graphical representation of the room is shown in **Fig. 4**.
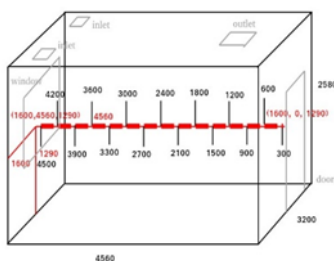

Fig. 4 - Schematic drawing and central line

3.3 Experiment 4: Breathing model

In this simulation, human breathing is simulated, see **Fig. 5** for the geometry. The following contour plots are taken from the other side, facing the mannequin. The groundwork for the breathing model is shown in 2.4.
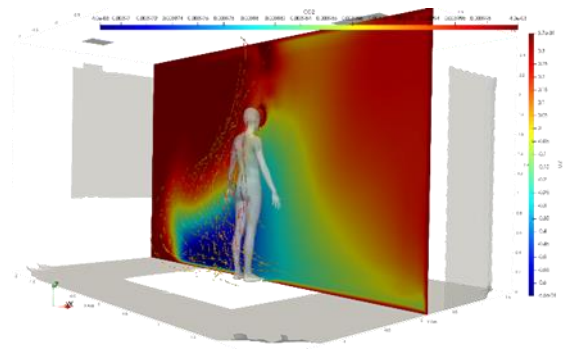

Fig. 5 - Visualization of simulation, the mannequin has a body temperature of 306.95[K], the exhaled air has a temperature of 309.15[K].

There are several reasons why it is interesting to simulate a mannequin with a realistic body temperature and breathing cycle.:

1. A realistic body temperature can be set, this will cause free convection and significantly alter the exposure.

2. By simulating the change of chemical content, CO2 levels will increase over time, another known gas with adverse health effects

3. The simulations that were generated before will be significantly different with density-driven free-convection, caused by the mannequin body temperature.

4. It requires more computational power to do these simulations, mainly because of the more complex geometry.

The mix of exhaled air needs to be adjusted, according to [20] the exhaled CO_2 concentrations under normal breathing are around $4 \approx 5\%$. The exhaled water content is also slightly higher, all increases in exhaled gas concentrations are deducted from the exhaled oxygen since this is the gas being used in the process. The mix for exhaled air is shown in **Tab. 2**.

Tab. 2 - Respired gas concentrations

Concentrations		
Gas	Respired	Gas
CO_2	4.0 %	CO_2
O_2	17.09 %	O_2
H_2O	1.5 %	H_2O

Fig. 6 shows the breathing cycle measured at the emitting surface. It can be seen that this can be used to determine exposure more realistically. The inhaled CO_2 can be calculated through equation (11), or directly through the breathing rate of $5.1[L \cdot min^{-1}]$ from **Fig. 2**.
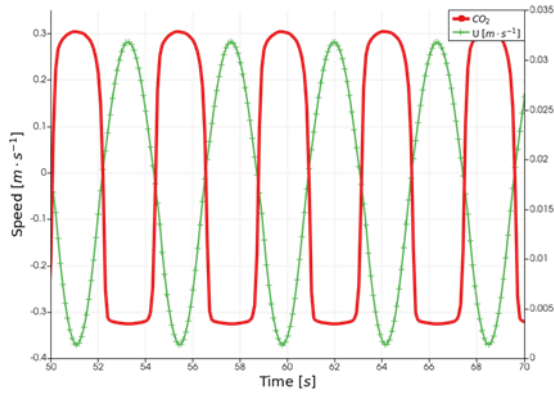
Fig. 6 - Speed U left, CO2 right. Note that the CO2 concentration fluctuates between 3.8% (exhaled) and 0.42% (inhaled)

$$\sum C_{gas,i} \cdot \Delta t_i \qquad (11)$$

The variable Δt_i in equation (11) stands for the time interval of the data, $C_{gas,i}$ denotes the specific gas concentration at that time. This can be applied only where the speed vector is negative, $U < 0$.

Fig. 7 shows the inhaled/exhaled gas concentration, these coincide perfectly with **Tab. 2**. Since the ozone concentration is initialized as zero, it can be observed that the concentration increases with each breathing cycle.
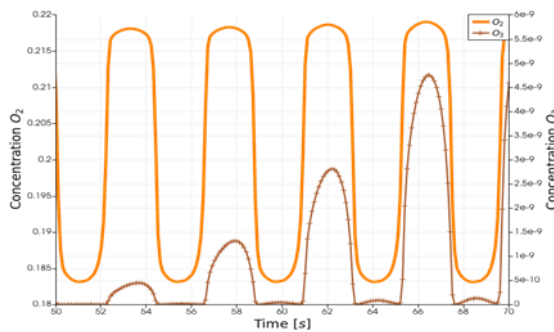

Fig. 7 - Inhaled/exhaled gas, Concentration oxygen left, ozone right. Note the difference in inhaled/exhaled oxygen.

Concentration over time

Fig. 8 shows how ozone and Limonene rapidly shoot up in the first time-steps. After around $25[s]$ the concentrations are high enough for the reaction towards C_{prod} to kick in.
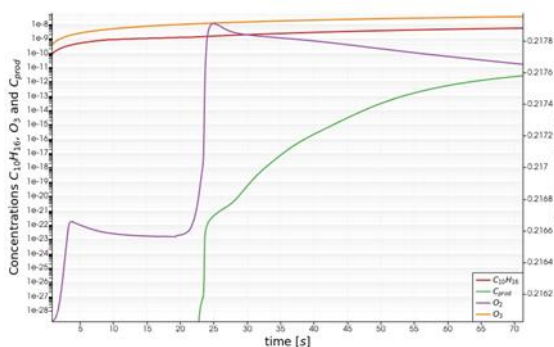

Fig. 8 - Note that the right axis of 3.10 is zoomed in, these initialization effects are less visible on larger scales.

Contour Plots

The contour plots shown below can be compared to the AEI contour plots to understand how concentrations and AEI relate. In **Fig. 9**, Higher concentrations of Ozone are visible close to the inlet and moving towards the person.
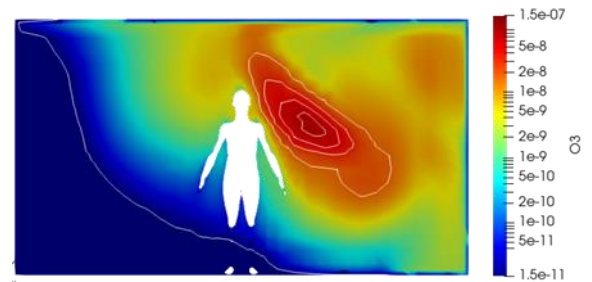

Fig. 9 - Ozone concentrations location Mid-Y

Fig. 10 shows high concentrations close to the emission surface at the floor and along with the mannequin towards the outlet, the simulated body temperature of the mannequin considerably aids convection, gas velocities close to the mannequin are up to $0.2[m \cdot s^{-1}]$ in the Z-direction.
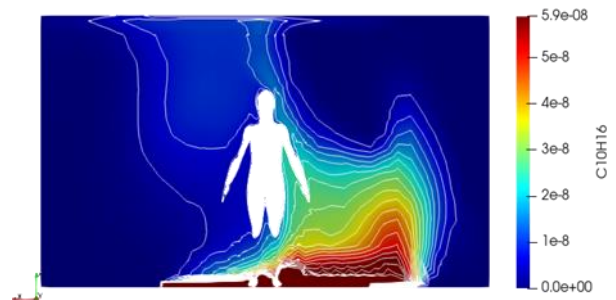

Fig. 11 - Limonene concentrations location Mid-Y

The CO_2 plot in **Fig. 12** is taken at the Inlet-1 surface, this visualizes the breathing better. It is noticeable that CO_2 tends to build-up closer to the inlet. Concentration differences are minimal, so the effect is small
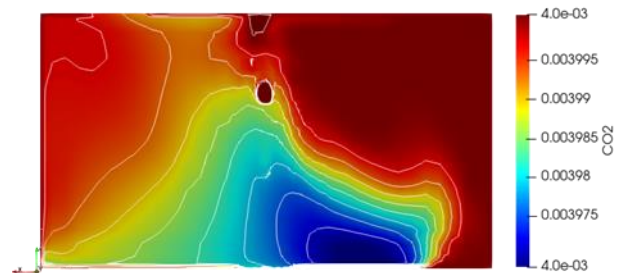

Fig. 12 - CO_2 concentrations location Mid-Y

3.3 Applying Adverse Effect Index

The matrix used is shown in **Fig. 13**. Because C_{prod} is a collection of species, it is roughly estimated that

C_prod consists largely of *IPOH*, *6−MHO* and *Acetaldehyde*[16], so the average of those 3 is taken, since information can be found in[11].

The steps explained in section 2.7 are still numerous if the total amount of gases mentioned in **Fig. 13** has to be processed.

Sum - Normalized AEI_rel		Effectgroup						
formula	Name	CHR	DEV	MGR	REP	SAC	SUB	Total Result
Cprod	C_Intermediate product	0.720	0.302	0.706	0.803	0.958	0.436	3.925	0.65
C10H16	D-Limonene	0.370	0.702	0.656		0.923	0.348	2.998	0.60
C10H16O2	3-Isopropenyl-6-oxo-heptanal	0.851	0.229	0.918	0.753	1.000	0.593	4.345	0.72
C8H14O	6-Methyl-5-hepten-2-one	0.871	0.134		0.753		0.397	2.155	0.53
CH2O	Formaldehyde	0.533	0.495	0.637		0.687	0.099	2.450	0.49
CH3CHO	Acetaldehyde	0.437	0.543	0.494	0.902	0.916	0.319	3.611	0.60
CO2	Carbon dioxide	0.010	0.379	0.626		0.770	0.184	1.969	0.3
N2	Nitrogen	0.196	0.711	0.951			0.468	2.325	0.58
O3	Ozone	0.408	0.431	0.770		0.768	0.383	2.760	0.55
	Total Result	3.676	3.623	5.051	2.409	5.064	2.790	22.613	
		0.488	0.436	0.7195	0.803	0.8603	0.3585		

Fig. 13 - AEI matrix weights used in the final calculation

For this reason, a python macro has been written for ParaView[6]. This script assumes you opened a .csv file in ParaView only containing a title header and the coefficients per gas and effect. It then asks the user for a comma-separated list of formula's to process, and it will apply the calculation.

3.4 final result

The method described in section 2.6 is now finally applied to the fourth simulation, **Fig. 14** shows the final result, the opacity of the planes and "clouds" are scaled to the applied AEI. The shown AEI is the fully collapsed version, where the average of all gases at that position is taken into account. The separate health effects per chemical are still available if desired.
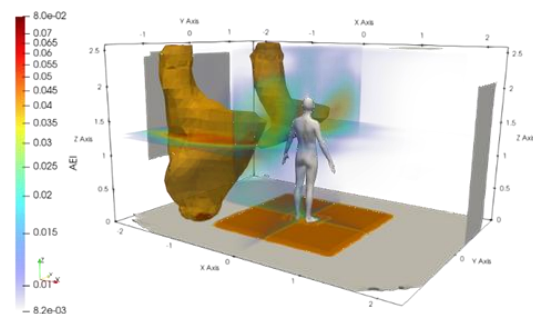

Fig. 14 – Opacity based on strength of AEI.

In **Fig. 14** it is visible that Ozone and Limonene cause the biggest hotspots, the orange blobs from the ceiling and at the floor have the lowest opacity and are most polluted. Note that it is very little, looking at the scale. But in relative terms this still holds. It stands out that lightly polluted blobs are visible around the mannequin. The slices in **Fig. 15** and **Fig. 16** show more clear where the hotspots are situated, primarily in front, behind and to the left of the mannequin. This is most likely caused by the positive updraft in the centre of the room, caused by simulated body temperature.
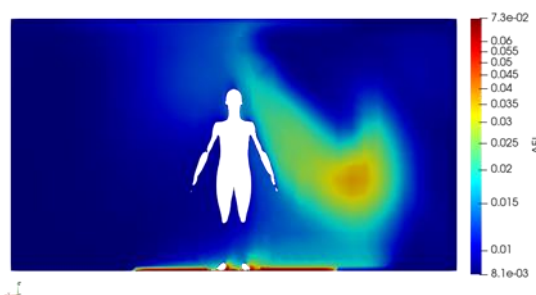

Fig. 15 - Adverse Effect Index location Mid-Y
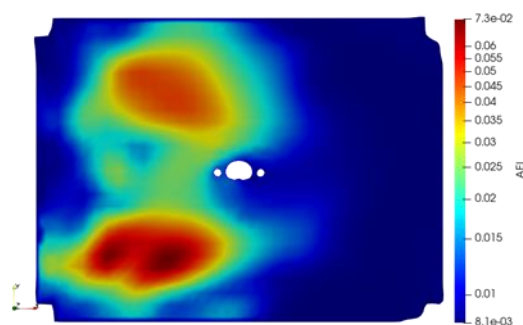

Fig. 16 - Adverse Effect Index, location Mid-Z

The blob to the left (shown on the right in **Fig. 15**) of the mannequin is primarily caused by C_{prod}, so this is the area where Limonene and Ozone first react. The 2 blobs in **Fig. 16** are caused by Ozone, coming down relatively straight down from the inlets. The areas in front of and behind the mannequin are caused by C_{prod} and CO_2.

4. Conclusion

4.1 discussion

1. A lot of data is missing, finding rate constants, Janaf coefficients, Sutherland coefficients or toxicity values like NOAEL are in general very hard to find.

2. the used database, genRA has many gaps and low p-values. For now, the results are unreliable.

3. Indoor gas-phase chemistry has not been studied as thorough yet as atmospheric chemistry, as a result, knowledge is taken from atmospheric chemistry, which leads to at best uncertainty for the moment.

4. A better categorization could be thought of for the Adverse Effect Index, or maybe a more flexible approach.

5. The AEI momentarily only says something about the *relative* toxicity within one set of data. If you want to compare 2 buildings, the data *must* be normalized and considered together as a whole.

Throughout the document, multiple problems were solved, which all build towards the modelling of the indoor environment in detail. In chapter 1 different kinds of simulations were considered, and the species of interest were selected. The decision was made to continue focusing on OpenFOAM because it

is free, well documented, capable and flexible. The chemicals Ozone, Formaldehyde and Limonene were selected as species of interest.

In chapter 2 different problems were solved to successfully apply an OpenFOAM model. First, the steep learning curve of CFD was undertaken and documented. Material (surface) emissions were determined and different ways to convert values from literature to OpenFOAM. To be able to simulate a breathing human, and the effects on the distribution of gases, a breathing model has been set up in section 2.4. Finally, the Adverse Effect Index, AEI was designed in section 2. A python script was developed for this purpose. The AEI builds on an online Generalized Read-Across toxicity database.

In Chapter 3, two simulations were executed. The first simulation was used as a validation tool, to prove that the selected OpenFOAM model performs well. The second simulation added a mannequin with a body temperature and simple breathing pattern, this model requires much finer mesh sizes and is ±100 times more computationally expensive compared to simulation 1.

Finally, the AEI was applied in section 3.3, a python macro script was developed for ParaView to apply the AEI fast and efficiently to any simulation with chemical concentrations that is accessible by ParaView. The results seem to be in line with the simulation and do provide a sane indication of healthier and less healthy spots within a given space.

5. Acknowledgement

6. References

[1] BOXMOX - box model extensions to KPP | Atmospheric Chemistry Observations & Modeling (ACOM).

[2] Council Directive 1999/13/EC of 11 March 1999 on the limitation of emissions of volatile organic compounds due to the use of organic solvents in certain activities and installations.

[3] Database for the Kinetics of the Gas-Phase Atmospheric Reactions of Organic Compounds – Eurochamp Data Center.

[4] Dirken, J. M. (Creator), Steenbekkers, L. P. A. (Creator), Daanen, .. (Creator), Voorbij, A. (Creator), Molenbroek, J. F. M. (. (Creator) (2018). Dutch adults (DINED - anthropometric database).

TU Delft - 4TU.ResearchData. 10.4121/UUID:1B214A8F-F59C-460F-8EB9-3EF8DB5E85EE

[5] Jenkin et al., Atmos. Environ., 31, 81, 1997 [doi:10.1016/S1352-2310(96)00105-7]

[6] Ahrens, James, Geveci, Berk, Law, Charles, ParaView: An End-User Tool for Large Data Visualization, Visualization Handbook, Elsevier, 2005, ISBN-13: 978-0123875822

[7] PubMed. https://pubmed.ncbi.nlm.nih.gov.

[8] Kim E. Barrett and William F. Ganong, editors. *Ganong's Review of Medical Physiology*. A Lange Medical Book. McGraw-Hill Med, 24. ed edition.

[9] Gabriel Bekö, Nicola Carslaw, Patrik Fauser, Violeta Kauneliene, Sascha Nehr, Gavin Phillips, Dikaia Saraga, Coralie Schoemaecker, Aneta Wierzbicka, and Xavier Querol. The past, present, and future of indoor air chemistry. 30(3):373–376.

[10] Alessandro D'Amico, Agnese Pini, Simone Zazzini, Daniela D'Alessandro, Giovanni Leuzzi, and Edoardo Currà. Modelling VOC Emissions from Building Materials for Healthy Building Design. 13(1):184.

[11] George Helman, Imran Shah, Antony J. Williams, Jeff Edwards, Jeremy Dunne, and Grace Patlewicz. Generalised Read-Across (GenRA): A workflow implemented into the EPA CompTox Chemicals Dashboard. 36(3):462–465.

[12] Kazuhide Ito, Masaru Abuku, Shinsuke Kato, and Shuzo Murakami. CFD and Model Experiment with Chemical Reaction.

[13] N. E. Klepeis, W. C. Nelson, W. R. Ott, J. P. Robinson,

[14] A. M. Tsang, P. Switzer, J. V. Behar, S. C. Hern, and W. H. Engelmann. The National Human Activity Pattern Survey (NHAPS): A resource for assessing exposure to environmental pollutants. 11(3):231–252, 2001 May-Jun.

[15] Yingjun Liu, Pawel K. Misztal, Caleb Arata, Charles J. Weschler, William W. Nazaroff, and Allen H. Goldstein. Observing ozone chemistry in an occupied residence. 118(6).

[16] Max R. McGillen, William P.L. Carter, Abdelwahid Mellouki, John J. Orlando, Bénédicte Picquet-Varrault, and Timothy J. Wallington. Database for the kinetics of the gas-phase atmospheric reactions of organic compounds.

[17] A. W. Nørgaard, J. D. Kudal, V. Kofoed-Sørensen, I. K. Koponen, and P. Wolkoff. Ozone-initiated VOC and particle emissions from a cleaning agent and an air freshener: Risk assessment of acute airway effects. 68:209–218.